Comparison of different CFD techniques for transient modelling of virtual breathing thermal manikins

Mijorski S.[1], Ivanov M.[2]

[1]PhD, SoftSim Consult Ltd., Consultant at Technical University of Sofia, FPEPM, Department: "Hydroaerodynamics and Hydraulic Machines", Sofia 1000, Bulgaria

[2]Senior Assist. Professor, PhD, Technical University of Sofia, FPEPM, Department: "Hydroaerodynamics and Hydraulic Machines", Sofia 1000, Bulgaria

*corresponding author: Martin Ivanov

e-mail: m_ivanov @tu-sofia.bg

Abstract

The presented paper reveals comparative analyses of three different CFD based transient modelling techniques (URANS, DES and LES) for flow simulations with virtual thermal manikins. The interaction between the simulated breathing flow and the free convection flow from the heated virtual manikin's surface for two breathing phases is performed under controlled room conditions. Recent studies of the authors' show that simulations under steady state conditions can lead to overprediction of the resultant fields, so the implementation of transient simulation methods is recommended in that case. Qualitative analyses between the different techniques are made, in terms of temperature and velocity fields' comparison. Considering that these virtual thermal manikins are modern complex tools for virtual design and assessment of the occupants' thermal comfort, as well as for virtual analyses of indoor air quality, the results achieved in the present study will provide new and valuable approach for the integration of various modelling techniques in the presented area. The CFD results has demonstrated a flow pattern similarities in both DES and LES solution methods, while in URANS simulations it was observed a deflection of the thermal plume with almost 0.4 m at 2.5 m height from the floor, under free convection conditions. Nevertheless, for the exhale phase of the breathing cycle, there was a good correlation between the different techniques, in the breathing zones of the manikin.

Keywords: CFD, URANS, DES, LES, Virtual Thermal Manikin, Breathing Flow Modelling

1. Introduction

The breathing thermal manikins are considered as very important tools in the environmental engineering practice. They represent accurate models of the human body and allow simulation of different levels of physical action, as well as some human activities such as breathing, sweating, sneezing, coughing and others. They are very complex instruments and are used also to study the convective flows around human bodies in different conditions, without excessive risk of exposure to the people themselves [*Madsen T. (1999*)]. However, experimental studies with real thermal manikins are expensive, time consuming, require highly skilled labour and are relatively difficult to conduct. Therefore, the use of Virtual Thermal Manikins (VTMs), particularly at the design and prediction stage of the indoor environment, seems to be appropriate alternative to the actual thermal manikins' experiments. Implementation of diverse Computational Fluid Dynamics (CFD) based simulation techniques is required to assess the performance level and accuracy of the created numerical models. Recent findings suggest that simulations under steady state conditions may over-predict the resulting parameter's impacts in the "breathing flow modelling" area [*Ivanov and Mijorski (2017)*]. It is suggested also that implementing transient conditions in these simulations will further improve the developed models of breathing VTMs. But implementing transient conditions in breathing flow and free convection flow modelling is not an easy task, and may require significant modelling skills and computational resources. The study of *Villafruela et.al. (2016)* summarizes that in the recent years, CFD simulation tools have been used to study the diffusion of inhaled and exhaled contaminants from different ambient environments. Also, complex airborne infection routes have been studied with CFD, including the sneezing and coughing mechanisms [*Villafruela et.al. (2016)*]. Steady-state breathing flow simulation study has been previously performed by the authors, to analyse the interaction between the inhaled/exhaled flow and the thermal plum characteristics, around the body of a thermal manikin [*Ivanov and Mijorski (2017)*]. Considering its nature, the breathing process in humans is transient, and the breathing flow parameters are changing completely and rapidly in relatively short period of time as demonstrated by the authors in [*Ivanov and Mijorski (2017)*]. This makes difficulties in the definition of boundary and initial conditions. But for accurate modelling, the breathing process should not be considered as steady-state and constant inhalation/exhalation velocity should not be assumed. Moreover, the convective flow around the thermal manikins is buoyancy driven, associated with high nonlinearities and fluctuations. In order to capture these effects in the presented study, three different transient techniques were implemented during the analysis:

- Unsteady Reynolds Averaged Navier Stokes (URANS): represents time-averaged equations of fluid

flow motion, decomposing the flow into its time-averaged and fluctuating quantities;

- Detached Eddies Simulations (DES): represents a hybrid method that treats near-wall regions with a Reynolds-Averaged Simulation (RAS) approach and the bulk flow with an LES approach;
- Large Eddies Simulations (LES): represents a method, where large turbulent structures in the flow are resolved by the governing equations, while all the smaller eddies filtered by the Sub-Grid Scales (SGS) are modelled.

The main aim of the presented paper is to perform comparison analyses of the described different CFD techniques for transient modelling of virtual breathing thermal manikins. The obtained results will provide significant understanding of the solution differences between less computational expensive methods like RAS and more advanced ones like LES and DES.

2. 3D model, spatial discretization and simulation setup

2.1. 3D Models

For the purpose of the presented study, it is used a polygonal virtual manikin model with appropriate structure and design, which meets the basic requirements of the ergonomic design area. The virtual manikin is designed by Georgi Chervendinev (*Engineering Design Lab at TU-Sofia*), in order to match the overall 95th percentile of the anthropometric size of a standard person. It has an approximate surface area of 2 m^2 and height of 1.75 m. The nasal valve opening is constructed according to the study of *Lin (2015)* and is shown in Fig. 1. The opening area of is 7.3 x 10^{-5} m^2. The normal to the nasal opening was specified to 45 degrees from the vertical body axis. Additionally, exhaust walls from the nasal valve to the nose end were inclined to 15 degrees according to the studies of *Nilsson (2006) and Lin (2015).*

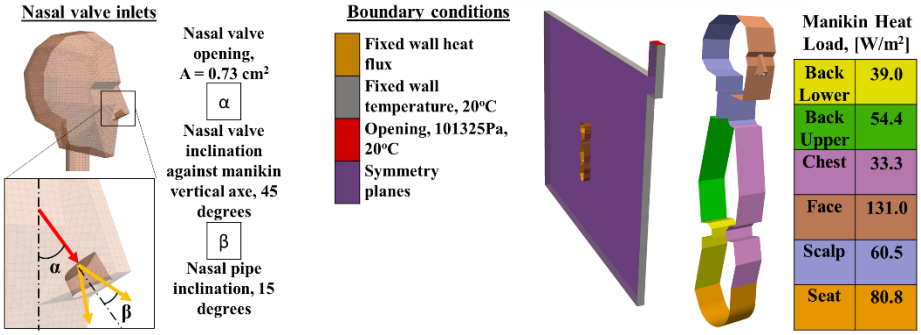

Figure 1. 3D model and CFD boundary conditions

2.2. Spatial discretization

For the purpose of the comparison analyses between the different CFD techniques, the computational domain was significantly reduced by introducing two symmetry planes, at the both sides of the manikin. This measure was considered with clear understanding of the flow restrictions that will be introduced, but with an aim of simulation time reduction. As shown on Fig. 1, the model comprised just 0.1 m section of the manikin, including the two nasal valve openings, head and manikin body, excluding the hands and legs. The 3D model of the polygonal thermal manikin is placed in the context of rectangular shaped room. The discretization was done with snappyHexMesh utility, part of an ENGYS® (*www.engys.com*) enhanced version of the CFD code OpenFoam® (*www.openfoam.com*). As a result, the numerical grid was with total of 670 000 poly-mesh control volume elements. The base cell size was defined to 2.5 10^{-2} m and to capture the nasal valve zones geometrical features the maximum level of cells refinement reached to 8 10^{-4} m. Additionally the manikin's surfaces were refined with the introduction of prism layers. By first layer height of 0.4 10^{-4} m, the y+ values over manikin surfaces were below 4 as recommended in the work of *Spalart (2001)*. Thus, the models matched the basic requirements of LES method for resolving accurately the turbulent flow over object surfaces.

2.3. Solution Methods

Three unsteady/transient 3D simulations were performed, covering two different phases of the human breathing cycle. These included no breathing or the free convection flow case for time duration of 20 seconds (allowing to get the solutions to a fully developed convective flow around the manikin and room space) and sequentially 2 seconds of exhale phase. In order to keep maximum Courant number below 1, the simulations were run with different time steps, as for former case it was set to $\Delta t = 1\ 10^{-3}$ seconds, while for the lather it was reduced to $\Delta t = 25\ 10^{-5}$ seconds. The solver for the transient buoyant turbulent flow of incompressible fluids *buoyantBoussinesqPimpleFoam* is used with combinations of PIMPLE algorithm for pressure-linking. The PIMPLE represents a merged Semi-Implicit Method for Pressure-Linked Equations (SIMPLE) and Pressure Implicit with Splitting of Operator (PISO) algorithms, thus offering an improved solution and faster convergence for the transient solutions. The URANS simulations were run with the Shear Stress Transport (SST) k-ω turbulence model initially proposed by *Menter (1993).* The model combines the k-ω approach in the inner parts of the boundary layer, but also switches to a k-ε approach in the free-stream regions of the computational domain. More details of the selected URANS turbulence model are given in the work of *Menter, (2011).* For the DES simulations, the Spalart-Allmaras turbulent model was implemented. Initially, the standard Spalart-Allmaras model was proposed by *Spalart and Allmaras (1994)*, and then its DES formulation was proposed by *Shur et al. (1999)*. The model uses the distance to the closest wall as

Table 1. Implemented boundary conditions

Boundary Name	Boundary Conditions	Inhale	Free convection flow	Exhale
No Slip Walls	Surface temperature, 20 [^{o}C]	Yes	Yes	Yes
Vent Opening	Temperature 20 [^{o}C] and pressure 101325 [Pa]	Yes	Yes	Yes
Manikin Surfaces	Fixed heat flux as per Fig.1	Yes	Yes	Yes
Nose inlet	Inlet flow rate, 6.29 10^{-3} [m^3/s] at 36 [^{o}C]	No	No	Yes
Symmetry	Symmetry plane	Yes	Yes	Yes

the definition for the length scale, which plays a major role in determining the level of production and destruction of turbulent viscosity of the flow. And finally, the LES simulations were run with k-equation eddy viscosity Sub-Grid-Scale (SGS) model formulation. The model is well described in the work of *Chai and Mahesh (2012)*. The one-equation eddy viscosity model for large-eddy simulation has an additional transport equation for SGS kinetic energy. The comparative assessment of the model with Direct Numerical Simulations (DNS) has shown good agreement in the derived results.

2.4. Initial and Boundary conditions

The fluid properties were specified for the reference conditions of the 101325 Pa and 20 ^{o}C air temperature. Thus the density was modified to 1.204kg/m^3; dynamic viscosity to 1.82 10^{-5} kg/(m.s); kinematic viscosity to 1.51 10^{-5} m^2/s and specific heat to 1006.0 J/(kg·K). Table 1 describes all the different boundary conditions adopted in the CFD models, while in Fig.1 are illustrated associated heat fluxes from the thermal manikin's surfaces. The heat fluxes were derived from the study of *Nilsson (2006)* on the basis of total heat load for whole manikin's surface of 110 W. The nasal valve openings were specified as velocity inlets for exhale phase, where the flow rate was calculated based on the study of *Lin (2015)*. The total flow rate for both nasal values were calculated to 1.26 10^{-2} m^3/s with fixed turbulent intensity of 6.8 %.

3. Results and discussion

The numerical results are presented in from of velocity and temperature plots for the free convection and exhale phases of the breathing cycle. Only one section of domain parallel to the symmetry plane is visualised (see Fig. 2 and 4). Additionally, graphical representations are given, illustrating a pointwise data. The first set of graphs shows the horizontal profiles above the manikin's head at different heights for free convection phase (no breathing) at the end of the 20th second (Fig. 3). Furthermore, the graph in Fig. 5 shows the maximum velocity measured at different distances from the nasal valve openings at the breathing zones of the manikin, calculated for the exhale phase at the end of the 2nd second of the solutions.

3.1. Free convections phase (no breathing)

During free convection breathing phase the flow around the thermal manikins is expected to be associated with low velocity buoyancy driven air fluctuations. This phenomenon is well visible in the transient flow solutions illustrated in Fig. 2. It is seen that, there is a good correlation in the temperature and velocity fields between different CFD techniques tested. The flow patterns of DES and LES solutions could be matched better, but also the URANS has demonstrated flow accelerations in the same zones of the modelled room. It should be pointed out the shifting back of the thermal plume with height change above the manikin head for both DES and LES methods. This is well visualised in Fig. 3, where for height change from 2.0 m to 2.3 m, there was almost 0.4 m difference of the thermal plume locations between URANS model results and the other two more advance techniques.

3.2. Exhale phase

The high dynamic characteristics of the flow in the breathing zone for the exhale phase are observed in the velocity and temperature plots on Fig.4. There is good visual agreement between different CFD techniques, with better mixing for DES and LES at the end of the exhaust jet of the manikin. Also, there is slight visible impact from the exhaust jet over the thermal plume zone above the manikin head. However, current set of results have only one exhale phase and it is expected this impact to increase after several breathing cycles. On Fig. 5, it is seen that the maximum velocity close to the nasal openings reaches 3.5 m/s for all the three cases. The graphical results show a good correlation in the exhale jets spreading in the breathing zone for all the three methods, but with a trend for higher velocity with model advancement. Thus, URANS model gives lowest air velocity levels, followed by DES method and LES, which is with the highest value. In all three cases, it is observed a flow decaying at 0.84 m away of the manikin's nasal valve.

4. Conclusions

Three different transient CFD techniques were assessed in the presented study. The comparison analysis has shown better correlation between DES and LES simulation results in both modelled breathing phases. However, the implementation of this two more advanced CFD techniques requires significantly higher computational resources compared to URANS. Also, these two methods are sensible to selection of boundary conditions, such as symmetry planes, which can alter the modelled flow by restricting large eddies generation. Despite the deflection of the thermal plume above the manikin's head, URANS

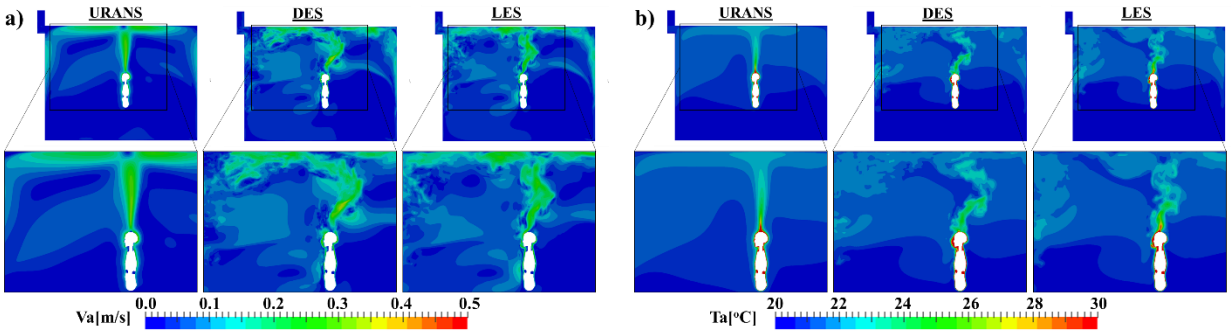

Figure 2. Free convection phase: a) Velocity fields; b) Temperature fields

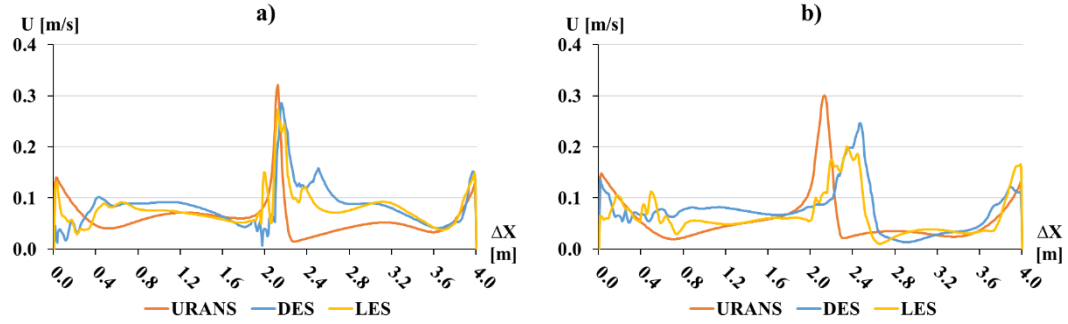

Figure 3. Horizontal velocity profile above manikin head for free convection breathing phase: a) 2.0 m height; b) 2.3 m height.

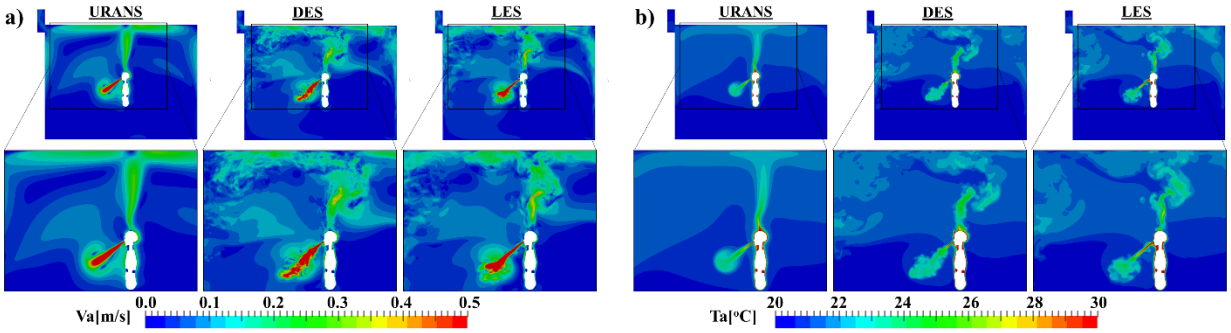

Figure 4. Exhale phase: a) Velocity fields; b) Temperature fields.

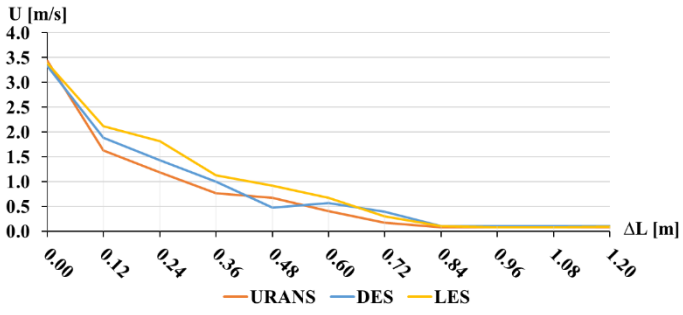

Figure 5. Maximum velocity measured at different distances from the nasal valve openings for exhale breathing phase.

simulations have demonstrated good results in the breathing zone for the exhale phase with slight underprediction of the air velocity.Also, the flow patterns in the room during free convection flow were matching closely the other two more advanced techniques. However, implementation of the URANS method should be done

with more carefulness and alertness, especially if model validations would be performed or discrete values would be derived.

Acknowledgements

The presented study is supported by “RDS” at TU-Sofia, as part of the activities under the "Perspective leaders" project, with Contract № 171ПР0016-02, entitled: “Implementation of CFD based intelligent technologies, for design assessment of developed virtual breathing thermal manikin".

References

Chai X., Mahesh K., (2012), “Dynamic k-equation model for large-eddy simulation of compressible flows”, Journal of Fluid Mechanics, vol. 699, pp. 385-413.

Ivanov M., Mijorski S., (2017), “CFD modelling of flow interaction in the breathing zone of a virtual thermal manikin”, “Energy Procedia” Journal, Volume 112, pp. 240-251, ISSN: 1876-6102, Elsevier;

Lin S., (2015), “Nasal Aerodynamics”, Chief Editor: Arlen D Meyers, MD, MBA, http: //emedicine. medscape.com/article/874822-overview#a1, Updated: May 14, 2015;

Madsen T., (1999), “Development of a breathing thermal manikin”, Proceedings of the 3rd international meeting on thermal manikin testing 3IMM, Stockholm, Sweden, 12–13 October;

Menter F., (1993), "Zonal Two Equation k-ω Turbulence Models for Aerodynamic Flows", AIAA Paper 93-2906;

Menter F., (2011), “Turbulence Modelling for Engineering Flows”, ANSYS Inc.;

Nilsson H., (2006) “How to Build and Use a Virtual Thermal Manikin Based on Real Manikin Methods”, Sixth International Thermal Manikin and Modelling Meeting”, “Thermal Manikins and Modelling”, ISBN: 962-367-534-8;

Shur M., Spalart P., Strelets M., Travin A, (1999), "Detached-Eddy Simulation of an Airfoil at High Angle of Attack", 4th International Symposium on Engineering Turbulence Modeling and Experiments, Corsica, France.

Spalart P. and Allmaras S., (1994), "A One-Equation Turbulence Model for Aerodynamic Flows," Recherche Aerospatiale, No. 1, pp. 5-21.

Spalart P., (2001), “Young-person’s guide to detached-eddy simulations grids”, NASA/CR-2001-21103, Boeing Commercial Airplanes, Seattle, Washington.

Villafruela J., Olmedo I., San Jose J., (2016), “Influence of human breathing modes on airborne cross infection risk”, Building and Environment 106, pp. 340-351